

Electronic Supplementary Information
Dithieno[3,2-b:2',3'-d]pyrrole-based Hole Transport Materials for
Perovskite Solar Cells with Efficiencies over 18%

*Sally Mabrouk,^b Mengmeng Zhang,^d Zhihui Wang,^{*c} Mao Liang,^{*a} Behzad Bahrami,^b*

*Yungen Wu,^a Jinhua Wu,^a Qiquan Qiao,^{*b} Shangfeng Yang^{*d}*

*^aTianjin Key Laboratory of Organic Solar Cells and Photochemical Conversion,
Department of Applied Chemistry, Tianjin University of Technology, Tianjin 300384,
P.R.China; *E-mail: liangmao717@126.com*

*^bCenter for Advanced Photovoltaics, Department of Electrical Engineering, South
Dakota State University, Brookings, South Dakota 57007, United States; *E-mail:
Qiquan.Qiao@sdstate.edu*

*^cJiangsu Provincial Key Laboratory of Palygorskite Science and Applied Technology,
College of Chemical Engineering, Huaiyin Institute of Technology, Jiangsu Province,
Huaian 223003, P. R. China; *E-mail: wangzhihui_tju@126.com*

*^dHefei National Laboratory for Physical Sciences at Microscale, Key Laboratory of
Materials for Energy Conversion, Chinese Academy of Sciences, Department of
Materials Science and Engineering, Synergetic Innovation Center of Quantum
Information & Quantum Physics, University of Science and Technology of China
(USTC), Hefei 230026, China; *E-mail: sfyang@ustc.edu.cn*

List of Contents

1. Materials and instruments	S3
2. Characterization	S3-6
3. Device fabrication	S6-7
4. Photovoltaic Performance Characterizations	S7-8
5. Synthesis	S8-10
6.The synthetic cost of H16	S11-14
Figure S1. The absorption coefficients for H16 ($12.1 \times 10^4 \text{ M}^{-1} \text{ cm}^{-1}$) and H18 ($9.8 \times 10^4 \text{ M}^{-1} \text{ cm}^{-1}$).....	S15
Figure S2. The cross-section view of the device based on H16.....	S15
Figure S3. The champion cells based on H16, H18 and spiro-OMeTAD.....	S16
Figure S4. Forward and reverse <i>J-V</i> characteristics of Spiro-OMeTAD (a), H16 (b) and H18 (c) based PSCs.....	S16
Figure S5. Thermogravimetric heating curves of H16 and H18 (heating rate $12 \text{ }^\circ\text{C min}^{-1}$ in N_2 atmosphere)	S17
Figure S6. Differential scanning calorimetry (DSC) curves of H16 and H18.....	S17
^1H and ^{13}C NMR spectra of compounds.....	S18-21
References	S22

EXPERIMENTAL SECTION

1. Materials and instruments

FAI, MABr, mesoporous TiO₂ (30NRD) and FK209 were purchased from Dyesol. PbI₂, PbBr₂ and CsI were ordered from TCI. Fluorine doped tin dioxide (FTO) coated glass substrates were obtained from Hartford Glass Company. Spiro-MeOTAD was purchased from the p-OLED (China). Lithium bis-(trifluoromethylsulfonyl)imide obtained from Sigma Aldrich.

2. Characterization

2.1 UV-Vis and CV measurements.

The absorption spectra of the solution of HTMs (dissolve in DCM) were measured using a SHIMADZU UV-2600 spectrophotometer. Fluorescence measurements were recorded by a HITACHI F-4500 fluorescence spectrophotometer. Cyclic voltammetry (CV) of these samples containing 0.1 M of tetrabutylammonium hexafluorophosphate (n-Bu₄NPF₆) was performed on a CHI660D electrochemical workstation in conjunction with a three-electrode electrochemical cell composed of a platinum electrode (counter electrode), Ag/AgCl electrode (reference electrode) and a glassy carbon disk (working electrode) at a scan rate of 10 mV s⁻¹. All potentials were reported against the ferrocene/ferrocenium (Fc/Fc⁺) reference.

2.2 Conductivity Measurements

Two-contact electrical conductivity set-up was used for measuring conductivities of the three HTMs. Samples were prepared using glass substrates cleaned via sonication

in soap water, DI-water, Acetone, then Isopropanol for 25 min, respectively. Thin layers of three HTMs were prepared by spin coating at 1000 rpm for 1 min from solutions with the same concentrations used for fabricating the devices. Finally, a 80 nm thick Ag back contact was deposited by thermal evaporation. The conductivity (σ) was determined by using eq.1 ¹.

$$\sigma = L / Rwd \quad (\text{eq. 1})$$

Here L is the channel length (0.05 mm), w is the channel width (0.2 μm), d is the thickness of HTM film. Thicknesses of the prepared films were measured with a DekTak profilometer, and R is the resistance.

2.3 Mobility Measurements

Hole mobility of the studied HTMs were recorded by space-charge-limited currents (SCLCs) according to previous literature ^{2,3}. Devices for mobility measurements are similar to those devices for J - V curves, but the TiO_2 layer was replaced by PEDOT:PSS. First, PEDOT:PSS was spin coated onto the substrates and then annealed on a hotplate at 120 °C for 30 min, forming a thin layer (< 100 nm). After that, HTMs were deposited via spin coating at 2000 rpm for 30 s. Finally, a 150 nm thick Ag back contact was deposited onto the HTM layer. The thicknesses of the HTMs were measured by using a Dektak profilometer. The current density of devices was measured with a Keithley 2400 Source-Measure unit. Hole mobility was calculated by the equations (2)

$$J = \frac{9}{8} \mu \epsilon_o \epsilon_r \frac{v^2}{d^3} \quad (2)$$

where J is the current density, μ is the hole mobility, ϵ_0 is the vacuum permittivity (8.85×10^{-12} F/m), ϵ_r is the dielectric constant of the material (approach 3), V is the applied bias, and d is the film thickness.

2.4 Topography and CS-AFM

Topography and current sensing atomic force microscopy (CS-AFM) of thin films of the HTMs were measured using Agilent SPM 5500 atomic force microscope equipped with MAC III controller (three lock-in amplifiers). A tip with resonance frequency of 67 kHz was used for measuring topography in non-contact mode. CS-AFM is a technique for the nanoscale electrical characterization of materials with high spatial resolution for measuring surface current using conducting Pt/Ir coated Si tip. The conducting tip scanned the film in contact mode and measured the variation in current across the surface with fixed bias. Carriers were injected from the conducting tip into the HTM and collected at the grounded FTO electrode. An in-built preamplifier with 1 nA V^{-1} sensitivity was used for measuring the current. The images were taken at 1 V bias to avoid oxidation/reduction of the tip and impurities on the surface of the film.

2.5 Transient Measurements

A Nitrogen Laser and a dye laser (Model 1011) were coupled resulting in a pump laser as the excitation source (pulse duration < 1 ns) for measuring transient of the fabricated devices. The pulse width was measured by oscilloscope through the response of the photodiode (spectral range 280 - 1100 nm). Charge transport time and

charge carrier lifetime obtained from transient photocurrent (TPC) and transient photovoltage (TPV). TPC was measured under short circuit conditions (by a very low resistor at 50 Ω) while TPV was measured under open circuit condition (by a huge resistor at 1 M Ω). Charge transport time and charge carrier lifetime were obtained by fitting the decay function with mono-exponential equation $A\exp(-t/\tau)$ where τ is the charge carrier life time. The obtained data were fitted with a mono-exponential decaying function to calculate charge transport time of the devices.

3. Device Fabrication

Perovskite solar cells were fabricated on fluorine-doped tin dioxide (FTO) coated substrates (1.5 cm \times 1.5 cm). FTO substrates were etched by diluted HCl solution (1 ml HCl in 10 ml DI water) and Zinc powder. The etched substrates were then cleaned via sonication in soap water, DI-water, acetone and isopropanol for 25 min, respectively, followed by treatment with oxygen plasma.

A thin layer of compact TiO₂ (0.15 M titanium diisopropoxide in ethanol) was spin coated at 4500 rpm for 45 sec followed by annealing at 200 $^{\circ}$ C for 10 min. A thin layer of mesoporous TiO₂ scaffolds was deposited by spin coating at 5000 rpm for 30 sec using a commercial TiO₂ paste (30 NRD, Dyesol) diluted in ethanol at a weight ratio of 1: 6 followed by annealing at 450 $^{\circ}$ C for 30 min. Substrates coated with TiO₂ are immersed in 25 mM TiCl₄ aqueous solution and annealed at 70 $^{\circ}$ C for 30 min followed by washing via DI water and ethanol, which was then annealed at 450 $^{\circ}$ C for 30 min.

Perovskite film was prepared according to the method reported by a previously work ⁴. The mixed perovskite precursor solutions contain FAI/PbI₂/MABr/PbBr₂ (mole ratio is 1/1.1/0.2/0.2) in anhydrous DMF/DMSO (v/v = 4/1). To improve the quality of perovskite film, CsI (1.5 M) was added to the above solution. The volume ratio of FAI/PbI₂/MABr/PbBr₂ and CsI is 5 / 95.

The mixed solution was stirred under 60 degree for an half of hour. A two-step program at 1000 and 6000 rpm for 10 and 30 s respectively was employed for spinning. During the second spinning process, a 100 μ L chlorobenzene was dripped on the substrate 15s before the coating is completed. Films with Cs-containing perovskite turned dark immediately after spin coating. The substrates were then annealed (usually at 100 °C) for 1 h in a nitrogen filled glove box.

After the perovskite annealing, the substrates were cooled down for few minutes and a Spiro-OMeTAD solution (70 nm in chlorobenzene) was spin coated at 4000 rpm for 20 s. Spiro-OMeTAD was doped with Li-TFSi and FK209 and TBP. The Spiro-OMeTAD additive molar ratios were 0.5, 0.03 and 3.3 for Li-TFSi, FK209 and TBP, respectively. Note that, the concentration of H16 and H18 is the same as that of Spiro-OMeTAD used. Samples were then transferred to the evaporator for Au deposition (80 nm) as the top electrode.

4. Photovoltaic Performance Characterizations

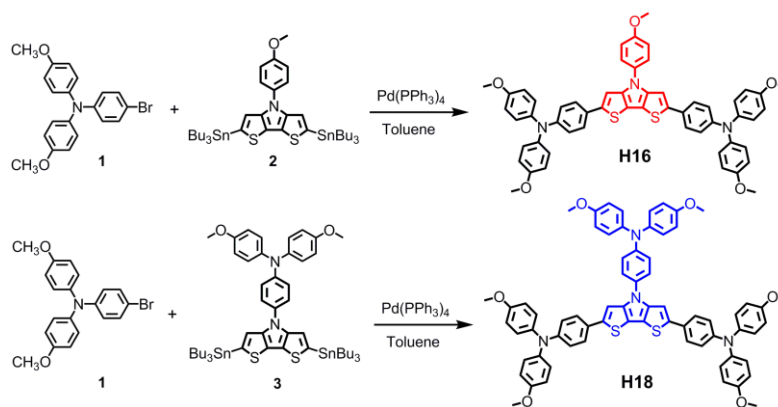
The current density–voltage ($J-V$) characterization of the devices was carried out by using a standard xenon-lamp-based solar simulator (Oriel Sol 3A, USA) under simulated AM 1.5 irradiation (100 mW·cm⁻²) with a digital source meter (Keithley

2400). The $J-V$ measurement was carried out under reverse scan with a scan rate of 0.1 V/s. At the same time, a measurement under forward scan was also performed for the devices to check the hysteresis of the $J-V$ curve. A NREL certified silicon reference cell (Oriel P/N 91150 V, with KG-5 visible color filter) was used as reference cell. All tests were carried out in air, and a mask with well defined area size of 14.0 mm² was attached onto the cell during test. Dozens of devices were fabricated and measured independently to obtain the statistical histograms of PCE devices. External quantum efficiency (EQE) was carried out with an ORIEL Intelligent Quantum Efficiency (IQE) 200 Measurement system established with the tunable light source.

5. Synthesis

¹H NMR and ¹³C NMR spectra were measured using Bruker AM-300/400 spectrometer. The chemical shifts were referenced from TMS. The mass spectra having high resolution were recorded using a Micromass GCT-TOF mass spectrometer. The synthetic routes for the H16 and H18 are shown in [Scheme S1](#).

4-(4-methoxyphenyl)-4H-dithieno[3,2-b:2',3'-d]pyrrole (MPDTP) and N-(4-(4H-dithieno[3,2-b:2',3'-d]pyrrol-4-yl)phenyl)-4-methoxy-N-(4-methoxyphenyl)aniline (TPDTP) were synthesized according to our previously work ⁵. All other solvents and chemicals used in this work were used as received from commercial suppliers without further purification.



Scheme S1. Synthetic routes to organic hole-transporting materials H16/H18.

Synthesis of Compound H16/H18

In a dried Schlenk tube was dissolved compound 4-(4-methoxyphenyl)-4H-dithieno[3,2-b:2',3'-d]pyrrole (MPDTP) or N-(4-(4H-dithieno[3,2-b:2',3'-d]pyrrol-4-yl)phenyl)-4-methoxy-N-(4-methoxyphenyl)aniline (TPDTP) (1 mmol) in anhydrous THF (10 mL), n-BuLi (0.88 mL, 2.5 mol/L) was added dropwise at $-78\text{ }^{\circ}\text{C}$ under argon atmosphere. The resulted mixture was stirred at the same temperature for one hour before $\text{Sn}(\text{But})_3\text{Cl}$ (780 mg, 2.2 mmol) was added. The remaining mixture was slowly warmed to room temperature and stirred overnight. The reaction was terminated by adding ice water, and the mixture was extracted with ethyl acetate and dried with anhydrous MgSO_4 . After the solvent was evaporated, the crude product **2/3** was obtained and used to synthesize compound H16/H18 without further purification.

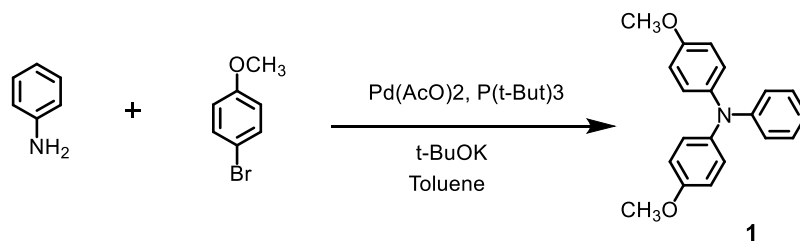
To a 100 mL two-neck round-bottom flask, a mixture of compound **2/3**, compound **1** (845 mg, 2.2 mmol), $\text{Pd}(\text{PPh}_3)_4$ (57 mg, 0.05 mmol) and toluene (10 mL) was added and heated at reflux for 8 hours under argon atmosphere. After evaporating the solvent

under reduced pressure, the remaining crude product was purified by column chromatography on silica gel eluted with DCM:PE = 1:15~2:1 (v/v) to afford the desired product H16/H18.

H16: Yellow solid, 65% yield for two steps. MP: 134-136 °C. ¹H NMR (400 MHz, (CD₃)₂CO): δ 7.58 (d, *J* = 8.8 Hz, 2H), 7.46 (d, *J* = 8.4 Hz, 4H), 7.35 (s, 2H), 7.11 (d, *J* = 8.8 Hz, 2H), 7.03 (d, *J* = 8.8 Hz, 8H), 6.89 (d, *J* = 8.8 Hz, 8H), 6.83 (d, *J* = 8.4 Hz, 4H), 3.87 (s, 3H), 3.77 (s, 12H). ¹³C NMR (100 MHz, (CD₃)₂CO): δ 159.9, 158.1, 149.9, 145.9, 143.9, 142.1, 134.1, 129.0, 128.4, 127.5, 126.1, 121.8, 116.6, 116.4, 116.3, 108.4, 56.7, 56.5. HRMS (ESI) calcd for C₅₅H₄₆N₃O₅S₂ (M+H⁺): 892.2879, found: 892.2783.

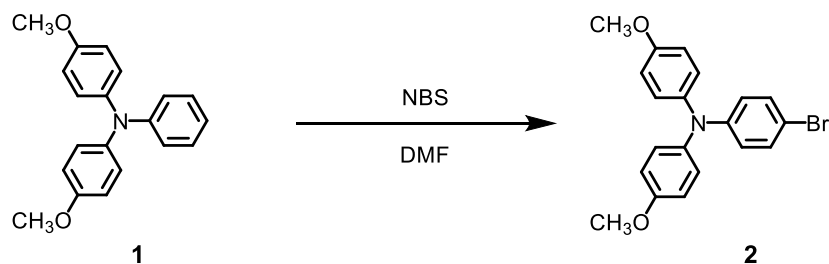
H18: Yellow solid, 65% yield for two steps. MP: 158-160 °C. White solid, 58% yield for two steps. ¹H NMR (400 MHz, (CD₃)₂CO): δ 7.43-7.39 (m, 6H), 7.33 (s, 2H), 7.08 (d, *J* = 8.8 Hz, 4H), 7.01 (d, *J* = 8.8 Hz, 8H), 6.97 (d, *J* = 8.8 Hz, 2H), 6.90-6.86 (m, 12H), 6.80 (d, *J* = 8.4 Hz, 4H), 3.76-3.75 (m, 18H). ¹³C NMR (100 MHz, (CD₃)₂CO): δ 158.2, 158.0, 149.8, 149.0, 142.2, 142.1, 133.5, 130.5, 129.8, 129.1, 128.6, 128.4, 127.5, 125.2, 122.1, 121.8, 116.5, 116.4, 108.6, 56.5. HRMS (ESI) calcd for C₆₈H₅₇N₄O₆S₂ (M+H⁺): 1089.3719, found: 1089.3785.

The synthetic cost of H16.



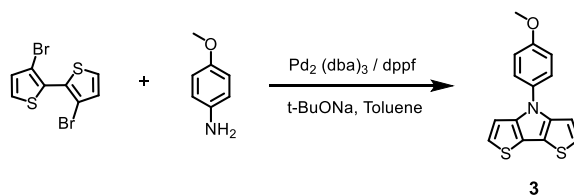
To a 100 mL two-neck round-bottom flask, a mixture of Aniline (2.3 g, 24.7 mmol), 4-Bromoanisole (10.2 g, 54.4 mmol), Pd(AcO)₂ (111 mg, 0.494 mmol), P(*t*-But)₃ (10% in Toluene, 2 g, 0.988 mmol), Potassium tert-butanolate (6.92 g, 61.75mmol) and toluene (35 mL) was added and refluxed overnight under argon atmosphere. After evaporating the solvent, the remaining crude product was purified by column chromatography on silica gel eluted with dichloromethane (DCM): petroleum ether (PE) = 1:15~1:5 (v/v) to afford the desired product **1** as an off-white solid (6.864 g, 91% yield).

Reagent	Amount / g	Amount / mL	Price / g or mL	Total price / RMB
Aniline	2.3		0.17	0.39
4-Bromoanisole	10.2		0.6	6.12
Pd(AcO) ₂	0.111		170	18.87
P(<i>t</i> -But) ₃ / 10% in Toluene	2.0		7.5	15
<i>t</i> -BuOK	6.92		0.53	3.67
Toluene		35	0.1	3.5
Silica gel	200		0.036	7.2
Petroleum ether 60-90 °C		1000	0.022	22
dichloromethane		150	0.02	3
Total cost	79.15 RMB			
Amount intermediate 1	6.864 g			
COST for intermediate 1	11.53 RMB/g			



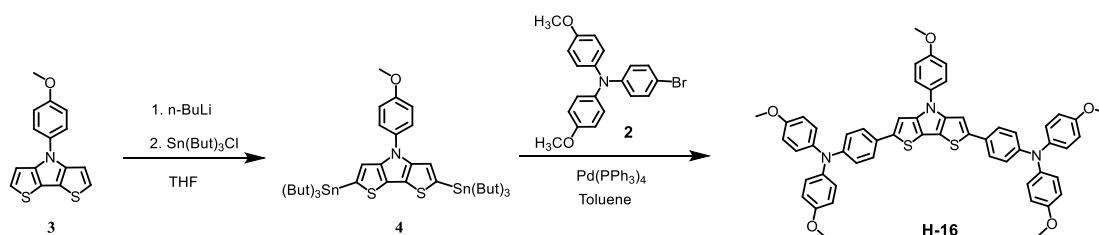
N-Bromo-succinimide (1.96 g, 11 mmol) was added in small portions to a solution of **1** (3.05 g, 10 mmol) in DMF (20 mL) and the obtained mixture was stirred for 2 h at room temperature. The reaction mixture was then poured into water and the obtained solid was filtered, washed with water and dried under vacuum. The collected crude product was purified by column chromatography on silica gel eluted with DCM: PE = 1:10~1:5 (v/v) to afford the desired product **2** as an off-white solid (3.639 g, 95% yield).

Reagent	Amount / g	Amount / mL	Price / g or mL	Total price / RMB
1	3.05		11.53	35.17
NBS	1.96		0.65	1.27
DMF		20	0.1	2
Silica gel	100		0.036	3.6
Petroleum ether 60-90 °C		300	0.022	6.6
dichloromethane		60	0.02	1.2
Total cost	49.84 RMB			
Amount intermediate 2	3.639 g			
COST for intermediate 2	13.7 RMB/g			



To a 100 mL two-neck round-bottom flask, a mixture of 3,3'-Dibromo-2,2'-bithiophene (1.62 g, 5 mmol), sodium *tert*-butoxide (1.92 g, 20 mmol), Pd₂(dba)₃ (46 mg, 0.05 mmol), dppf (112 mg, 0.2 mmol) and anhydrous toluene (20 mL) was added and stirred at room temperature for 5 minutes under argon atmosphere. Then, p-Anisidine (0.8 g, 6.5 mmol) was added, the resulting mixture was heated at reflux overnight. After evaporating the solvent, the remaining crude product was purified by column chromatography on silica gel eluted with DCM: PE = 1:25~1:10 (v/v) to afford the desired product **3** as a light yellow solid (1.144 g, 80% yield).

Reagent	Amount / g	Amount / mL	Price / g or mL	Total price / RMB
3,3'-Dibromo-2,2'-bithiophene	1.62		68.5	110.97
p-Anisidine	0.8		0.436	0.35
Pd ₂ (dba) ₃	0.046		90	4.14
dppf	0.112		4.85	5.43
<i>t</i> -BuONa	1.92		0.4	0.77
Toluene		20	0.1	2
Silica gel	100		0.036	3.6
Petroleum ether 60-90 °C		300	0.022	6.6
dichloromethane		20	0.02	0.4
Total cost	134.26 RMB			
Amount intermediate 3	1.144 g			
COST for intermediate 3	117.36 RMB/g			



In a dried Schlenk tube was dissolved compound **3** (286 mg, 1 mmol) in anhydrous THF (10 mL), n-BuLi (0.88 mL, 2.5 mol/L) was added dropwise at $-78\text{ }^{\circ}\text{C}$ under argon atmosphere. The resulting mixture was stirred at the same temperature for one hour before $\text{Sn}(\text{But})_3\text{Cl}$ (780 mg, 2.2 mmol) was added. The remaining mixture was slowly warmed to room temperature and stirred overnight. The reaction was terminated by adding ice water, and the mixture was extracted with ethyl acetate and dried with anhydrous MgSO_4 . After the solvent was evaporated, the crude product **4** was obtained and used to synthesize H16 without further purification.

To a 100 mL two-neck round-bottom flask, a mixture of compound **4**, compound **2** (845 mg, 2.2 mmol), $\text{Pd}(\text{PPh}_3)_4$ (57 mg, 0.05 mmol) and toluene (15 mL) was added and heated at reflux for 8 hours under argon atmosphere. After evaporating the solvent under reduced pressure, the remaining crude product was purified by column chromatography on silica gel eluted with $\text{DCM}:\text{PE} = 1:15\sim 2:1$ (v/v) to afford the desired product H16 as a yellow solid (0.581 g, 91% yield for two steps).

Reagent	Amount / g	Amount / mL	Price / g or mL	Total price / RMB
3	0.286		117.36	33.56
n-BuLi (2.5mol / L)		0.88	0.4	0.352
$\text{Sn}(\text{But})_3\text{Cl}$	0.781		1.69	1.32
THF		10	0.6	6

2	0.845		13.7	11.58
Pd(PPh ₃) ₄	0.057		44	2.51
Toluene		15	0.1	1.5
Silica gel	200		0.036	7.2
Petroleum ether 60-90 °C		1000	0.022	22
dichloromethane		1000	0.02	20
Total cost	106.02 RMB			
Amount H16	0.581 g			
COST for H16	182.48 RMB/g			

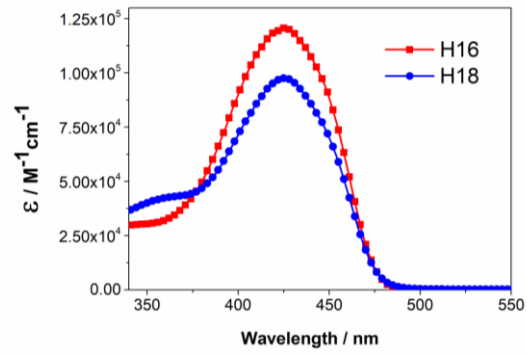


Figure S1. The absorption coefficients for H16 ($12.1 \times 10^4 \text{ M}^{-1} \text{ cm}^{-1}$) and H18 ($9.8 \times 10^4 \text{ M}^{-1} \text{ cm}^{-1}$).

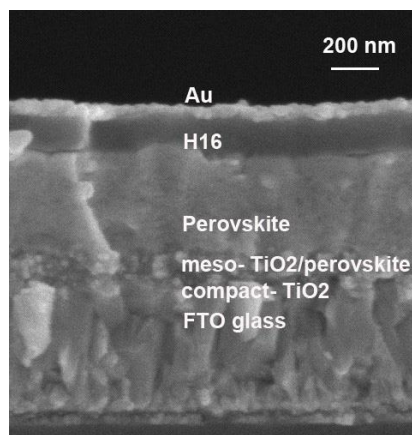


Figure S2. The cross-section view of the device based on H16.

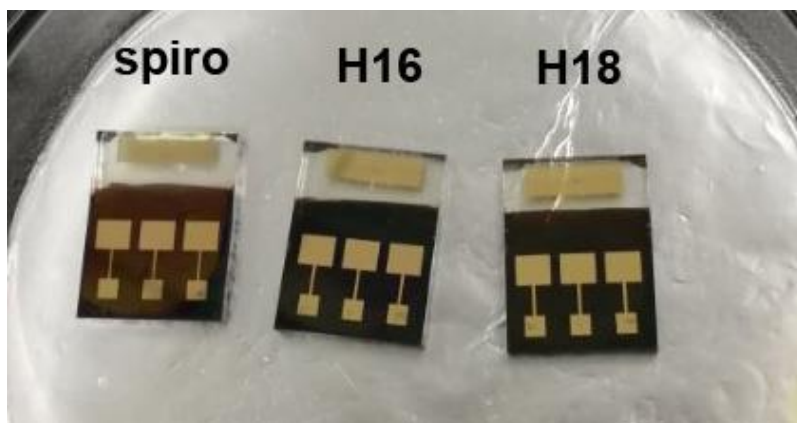


Figure S3. The champion cells based on H16, H18 and spiro-OMeTAD.

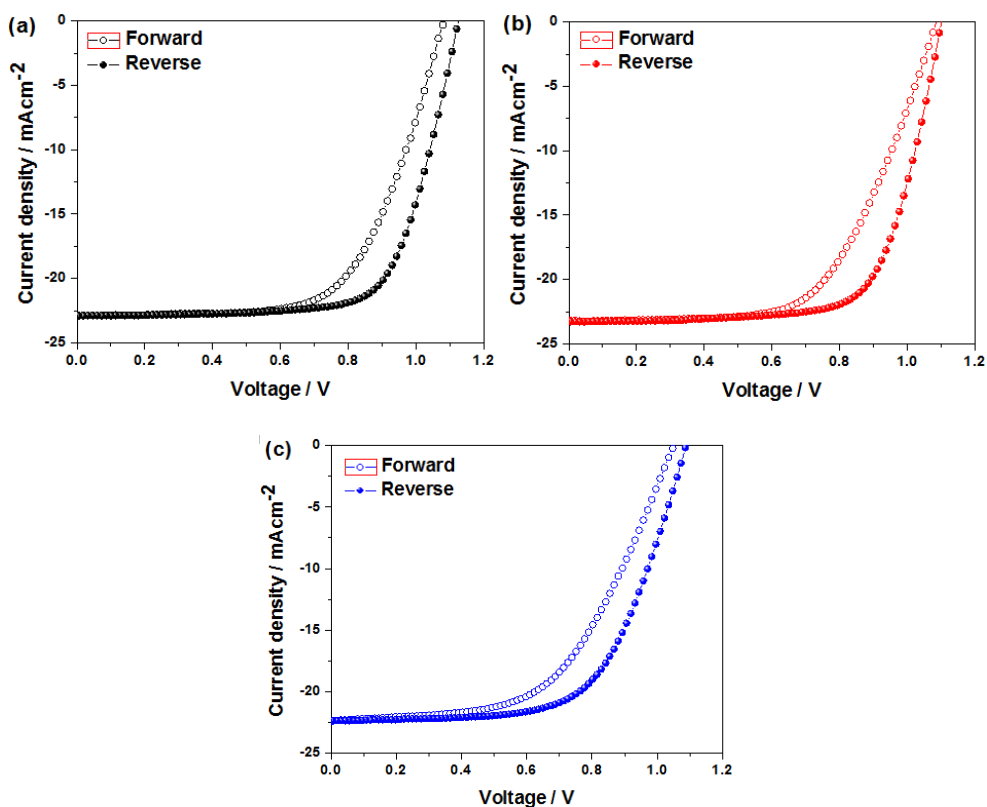


Figure S4. Forward and reverse J - V characteristics of Spiro-OMeTAD (a), H16 (b) and H18 (c) based PSCs.

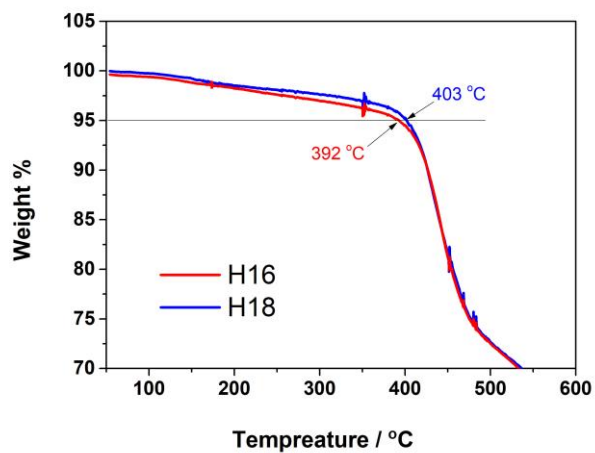


Figure S5. Thermogravimetric heating curves of H16 and H18 (heating rate 12 °C min⁻¹ in N₂ atmosphere).

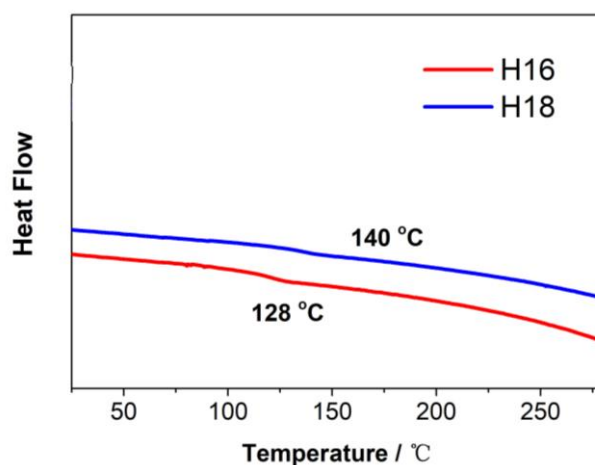
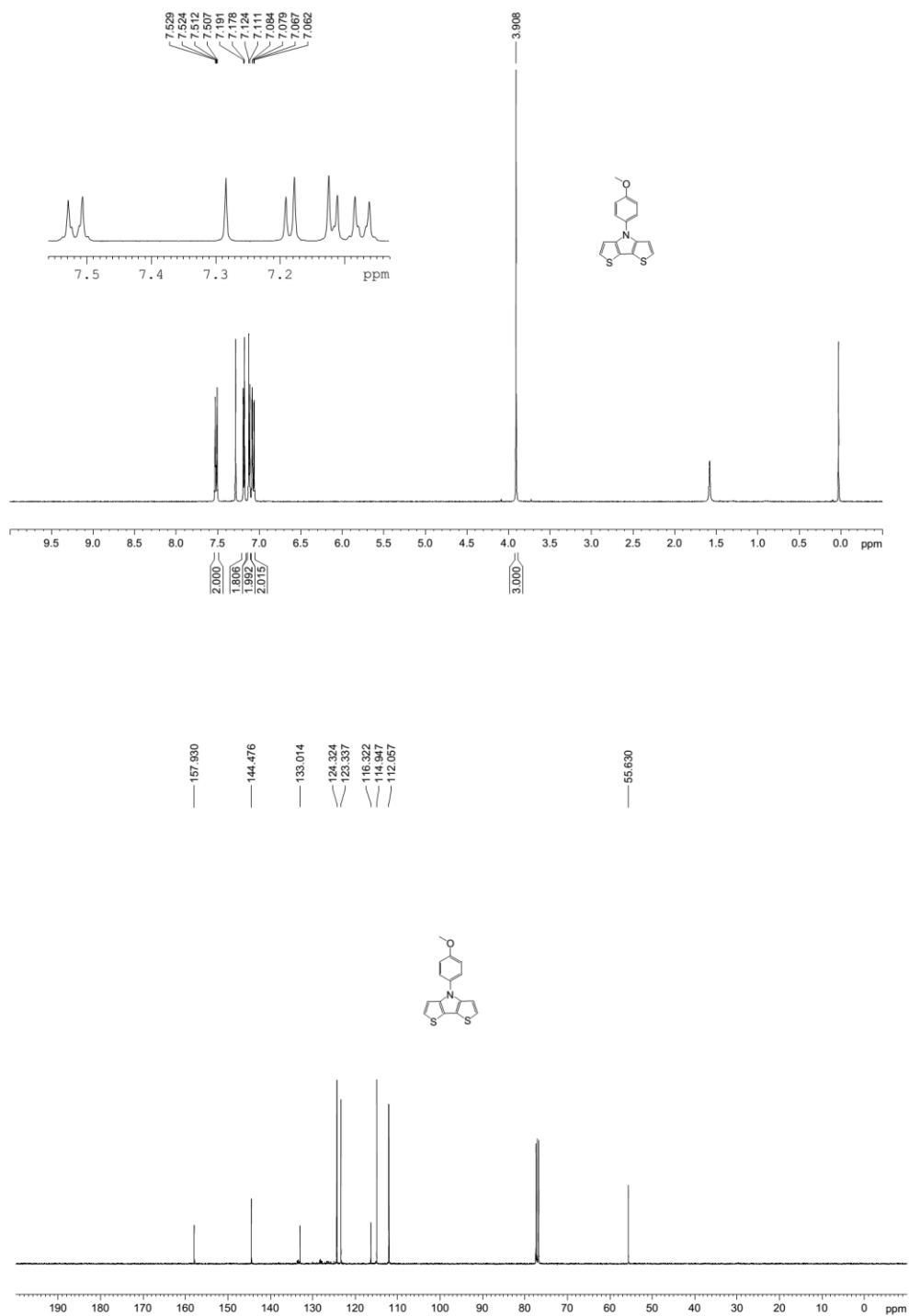
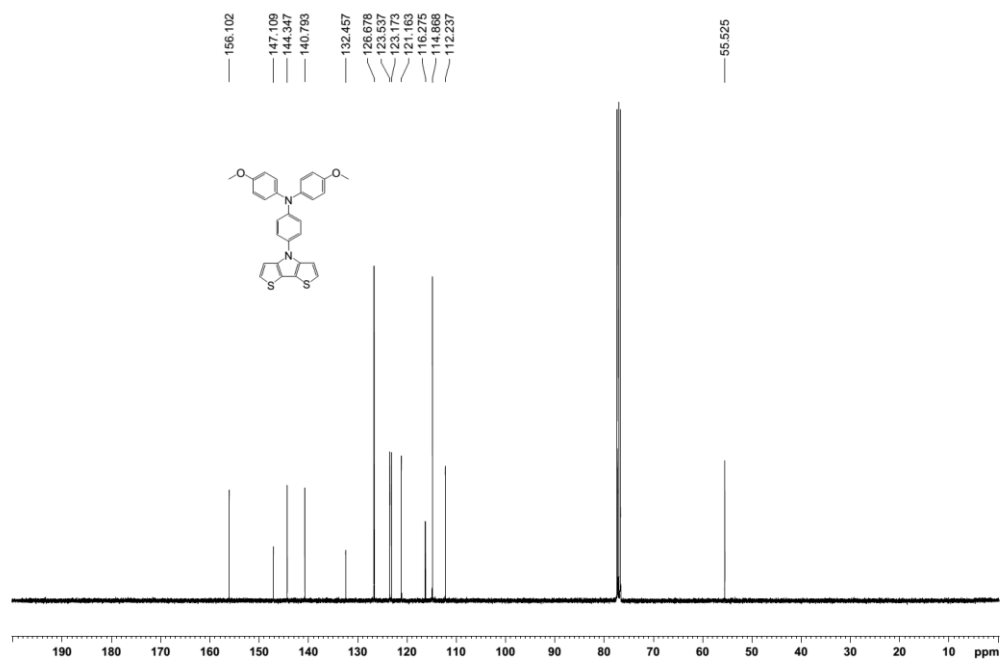
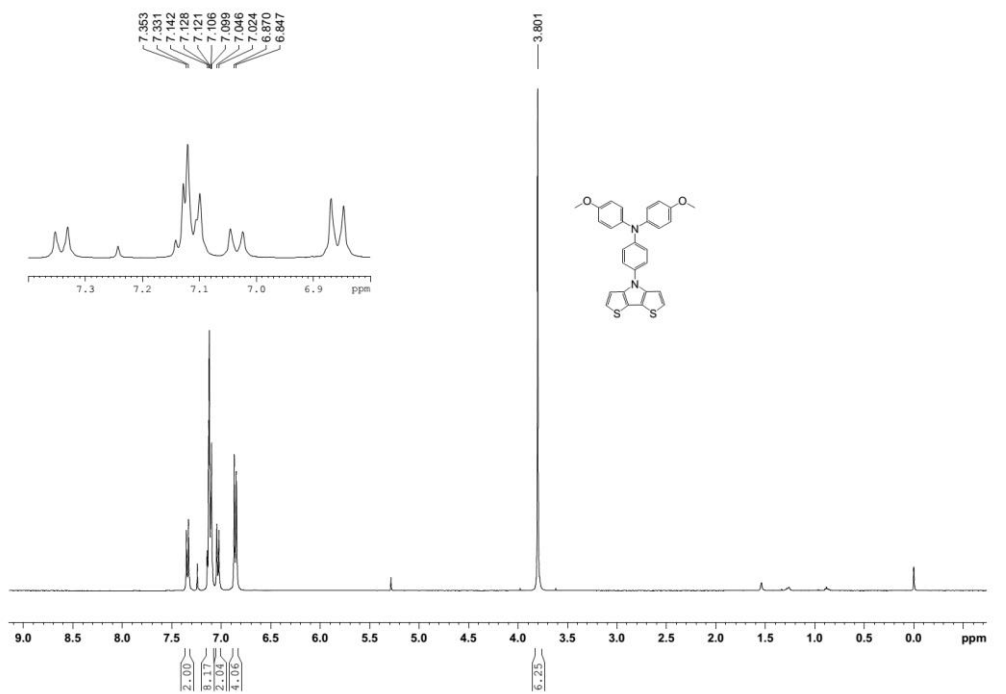


Figure S6. Differential scanning calorimetry (DSC) curves of H16 and H18. The T_g of H16 and H18 was determined to be 128 °C and 140 °C.

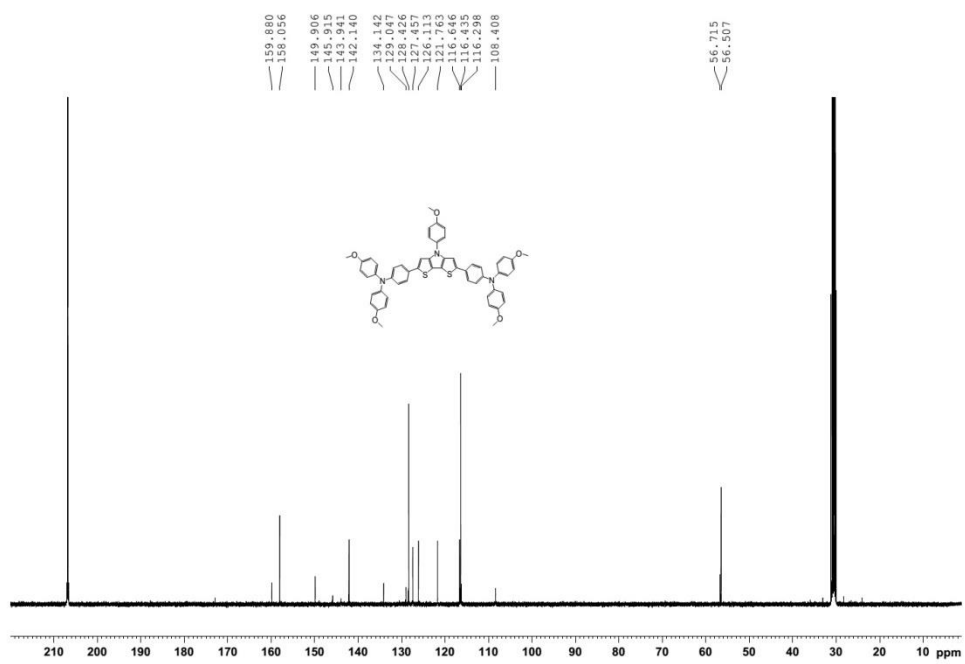
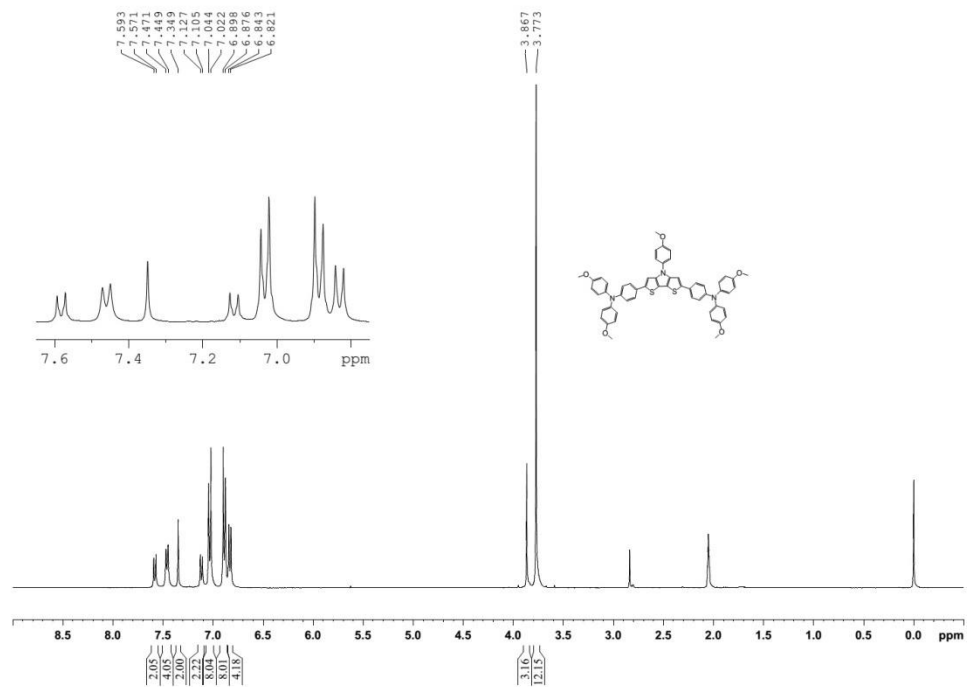
^1H and ^{13}C NMR (CDCl_3) spectra of compound
4-(4-methoxyphenyl)-4H-dithieno[3,2-b:2',3'-d]yrrole (MPDTP)



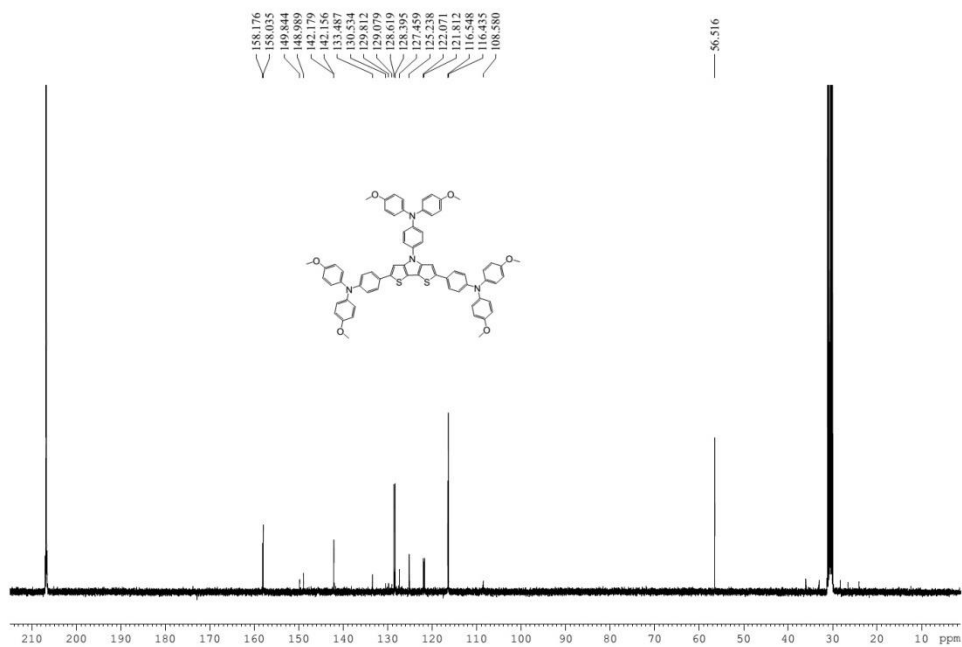
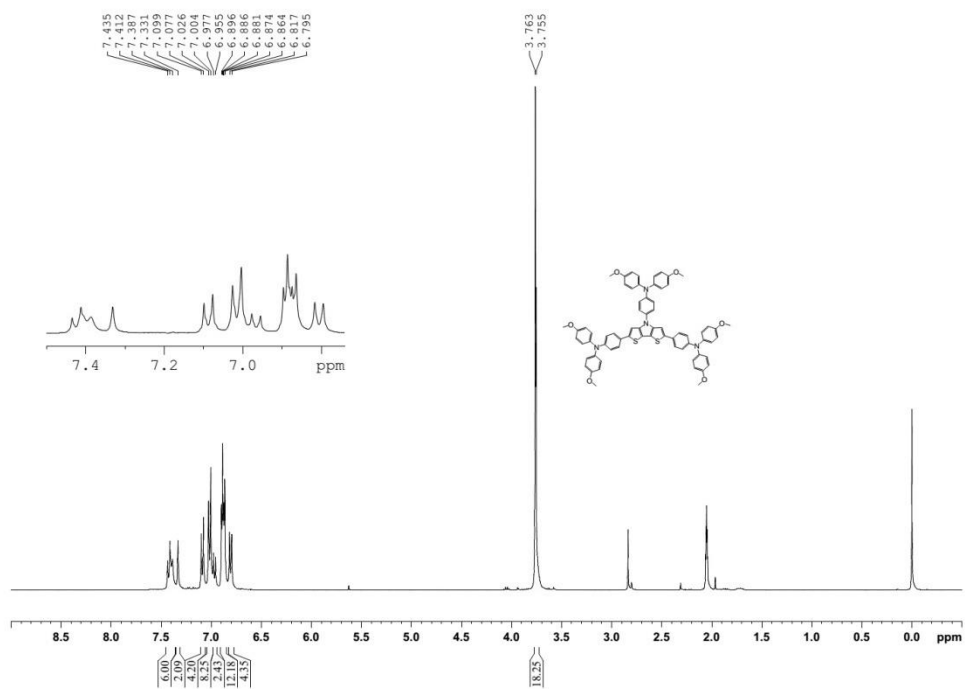
^1H and ^{13}C NMR (CDCl_3) spectra of compound N-(4-(4H-dithieno[3,2-b:2',3'-d]pyrrol-4-yl)phenyl)-4-methoxy-N-(4-methoxyphenyl)aniline (TPDTP)



^1H and ^{13}C NMR (d_6 -Acetone) spectra of compound H16



^1H and ^{13}C NMR (d_6 -Acetone) spectra of compound H18



References

1. H. J. Snaith and M. Grätzel, *Appl. Phys. Lett.*, 2006, **89**, 262114.
2. B. Xu, E. Sheibani, P. Liu, J. Zhang, H. Tian, N. Vlachopoulos, G. Boschloo, L. Kloo, A. Hagfeldt and L. Sun, *Adv. Mater.*, 2014, **26**, 6629-6634.
3. D. Bi, B. Xu, P. Gao, L. Sun, M. Grätzel and A. Hagfeldt, *Nano Energy*, 2016, **23**, 138-144.
4. M. Saliba, T. Matsui, J.-Y. Seo, K. Domanski, J.-P. Correa-Baena, M. K. Nazeeruddin, S. M. Zakeeruddin, W. Tress, A. Abate and A. Hagfeldt, *Energy Environ. Sci.*, 2016, **9**, 1989-1997.
5. Z. Wang, M. Liang, L. Wang, Y. Hao, C. Wang, Z. Sun and S. Xue, *Chem. Commun.*, 2013, **49**, 5748-5750.